

Characterization of Cross-Line up to 110 GHz Using Two-Port Measurements

Korkut Kaan Tokgoz, Shotaro Maki, Kenichi Okada, Akira Matsuzawa

Department of Physical Electronics
Tokyo Institute of Technology
Tokyo, Japan
korkut@ssc.pe.titech.ac.jp

Abstract—Cross-line, a four-port device, used for capacitive cross coupling in differential millimeter-wave amplifiers is modeled and characterized up to 110 GHz using two-port vector network analyzer measurement results. This passive component is electrically symmetrical to be used in differential amplifiers for decreased amplitude and phase mismatch. Two characterization structures are used for the method to be applied. The results are compared with four-port measurements up to 67 GHz. The comparisons show good agreement between the two methods.

Keywords—capacitive cross coupling, characterization, CMOS, reduced port measurements, mm-wave

I. INTRODUCTION

Millimeter-wave frequency region is one strong candidate for tens of gigabits per second data rate communications. The 9 GHz unlicensed band in 60 GHz frequency is such example to achieve high data rate wireless transceivers. Moreover, among several manufacturing technologies CMOS is very advantageous in terms of cost and monolithic implementation with analog and digital baseband circuitry [1]. The very first step to implement a CMOS transceiver working successfully, starts with millimeter-wave process design kit (PDK) development, a necessary step for accurate designs especially considering transceivers with high order modulations. This development phase includes active and passive devices. Moreover, two- or more than two port devices have to modeled and characterized. Cross-line device, the main focus of this work, is a four-port device, which is illustrated in Fig. 1. This device is intended to be symmetrical and reciprocal in order to be used in differential capacitive cross coupled millimeter-wave CMOS amplifiers for decreased amplitude and phase mismatch between the differential signals [2]. The four-port characterization of this device along with differential de-embedding procedures are explained in detail in [2]. One of the main issues about this procedure is the accuracy of differential de-embedding procedures compared to two-port de-embedding ones. In the differential de-embedding the coupling effects between probe tips are not negligible especially very high frequencies. Addition to this fact, the dynamic range of the measurement equipment for four-port version is less than two-port version. One other issue about the above mentioned method is that the characterization cannot be done up to 110 GHz since our own four-port VNA can work up to 110 GHz. It is better to note that in many industrial and academic institutions most common VNA is the two-port one [3]. For these reasons, in here an accurate characterization method

based on two-port VNA measurement results are introduced for the cross-line. In the next section, the cross-line and its properties are introduced along with the characterization structures. In section III, the method is provided for the characterization. Before the conclusion, in section IV the experimental results are provided along with a comparison with the previous characterization results mentioned in [2].

II. CHARACTERIZATION STRUCTURES

The cross-line is illustrated in Fig. 1. The dark gray areas represent the top metal layer and the black areas represent a lower metal layer, which is used for thru connection of port 1 and 4, and 2 and 3. The overall area of cross line is 20 μm by 20 μm . This passive device is electrically symmetrical and reciprocal as already mentioned before. Considering the properties, the four-port S-parameters can be simplified as follows;

$$S_C = \begin{bmatrix} S_{11} & S_{21} & S_{31} & S_{41} \\ S_{21} & S_{11} & S_{41} & S_{31} \\ S_{31} & S_{41} & S_{11} & S_{21} \\ S_{41} & S_{31} & S_{21} & S_{11} \end{bmatrix} \quad (1)$$

The number of unknowns from this assumption is four, which are S_{11} , S_{21} , S_{31} , and S_{41} . Two different characterization structures are enough for accurate characterization after a careful considerations for two-port measurements. The structures are provided in Fig. 2. In both structures cross-line is used four times. Basically, there are two important reasons behind this. The first one is that the pad to pad distance should be around 200 μm to avoid cross-talk between probe tips. The other reason is that using several times would decrease possible errors from de-embedding and transmission line modeling which are needed for characterization. Fig. 2(a) represents the characterization structure used open circuit as termination for the unused ports of the device.

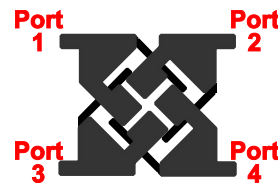


Fig. 1. Illustration of cross-line designed for differential amplifiers. Dark gray areas show top metal layer and black areas show a lower metal layer used for thru connections of port 1 to 4 and port 2 to 3.

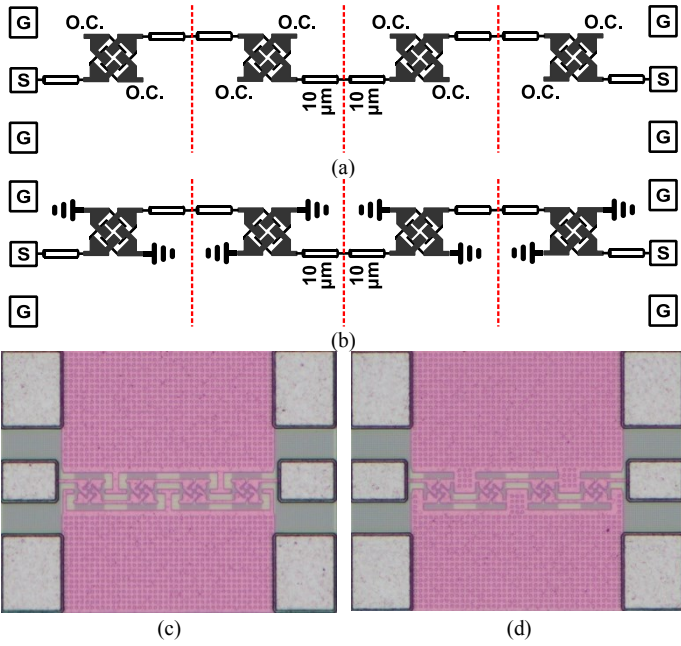


Fig. 2. Characterization structures for cross-line in each structure cross-line is repeated four times, and either ports 2 and 3 are terminated or ports 1 and 4 are terminated (a) characterization structure with open circuited (O.C.) terminations used, (b) characterization structure with short circuited terminations used, (c) chip photo of (a), and (d) chip photo of (b).

Moreover, Fig. 2(b) represents the short circuited version for the unused ports. The chip photos of the characterization structures are shown in Fig. 2(c) and (d) for open and short circuited terminations, respectively. Transmission lines with a length of $10\ \mu\text{m}$ are connected to the unterminated ports of the devices. The leftmost and rightmost devices are connected to measurement pads. In both structures, either ports 1 and 4 or 2 and 3 are terminated. Basically, they provide the same resultant S-parameters. This can be proved starting from the following equation [3], [4];

$$\mathbf{S}_{\text{Reduced}} = \mathbf{S}_{JJ} + \mathbf{S}_{JK}(\mathbf{\Gamma}_{KK}^{-1} - \mathbf{S}_{KK})^{-1}\mathbf{S}_{KJ} \quad (2)$$

Note that all of the bold characters in the above equation represent a two-by-two matrix. $\mathbf{S}_{\text{Reduced}}$ is the two-port S-parameter of the terminated four-port device. The subscripts JJ is for the unterminated ports, and KK is for the terminated ports. For instance, when ports 2 and 3 is terminated for the device mentioned here JJ is 1 and 4, and KK is 2 and 3. The subscripts JK and KJ is the related S-parameters between the terminated and unterminated ports of the device. It is mentioned that either termination of ports 1 and 4 or ports 2 and 3 result in the same S-parameters, because in either case the related matrices are same as provided below;

$$\mathbf{S}_{JJ} = \mathbf{S}_{KK} = \begin{bmatrix} S_{11} & S_{41} \\ S_{41} & S_{11} \end{bmatrix} \quad (3)$$

$$\mathbf{S}_{JK} = \mathbf{S}_{KJ} = \begin{bmatrix} S_{21} & S_{31} \\ S_{31} & S_{21} \end{bmatrix} \quad (4)$$

Moreover, in both case the ports are terminated with same reflections either open circuit or short circuited, for which the related termination matrices ($\mathbf{\Gamma}_{SS}^{-1}$ is for short circuited and $\mathbf{\Gamma}_{OO}^{-1}$ is for open circuited terminations) can be given as follows;

$$\mathbf{\Gamma}_{OO}^{-1} = \begin{bmatrix} 1 & 0 \\ 0 & 1 \end{bmatrix} \quad (5)$$

$$\mathbf{\Gamma}_{SS}^{-1} = \begin{bmatrix} -1 & 0 \\ 0 & -1 \end{bmatrix} \quad (6)$$

It can be considered that terminating ports 1 and 2, and 3 and 4 would be a similar idea for characterization structure generation and the results can be calculated similarly which is explained in the next section. It is true however, the values of S-parameters between ports 1 and 2, and 3 and 4 are coupling and they are very small which would result in decreased accuracy. That is why in this work; pairs of ports 1 and 4, and 2 and 3 are selected. In the next section the full four-port S-parameters calculations are introduced with the method.

III. METHOD OF CHARACTERIZATION

After measuring the two characterization structures (Fig. 2(c) and (d)) with a two-port VNA up to 110 GHz, the de-embedding of pad responses have to be done. Note that the pads and transmission lines are characterized beforehand of this work as in [5]. The remaining responses for the measurement results can be given as in the following equations in terms of T-parameters.

$$\mathbf{T}_{MO} = \mathbf{T}_{LP}\mathbf{T}_{CLO}^4\mathbf{T}_{RP} \quad (7)$$

$$\mathbf{T}_{MS} = \mathbf{T}_{LP}\mathbf{T}_{CLS}^4\mathbf{T}_{RP} \quad (8)$$

\mathbf{T}_{MO} is the T-parameters for the measured structure in Fig. 2(a) where open circuit is used for terminations. Similarly, \mathbf{T}_{MS} is the T-parameters for the measured structure in Fig. 2(b) where short circuit is used for terminations. \mathbf{T}_{LP} and \mathbf{T}_{RP} are the T-parameters for the left and right pads. \mathbf{T}_{CLO} and \mathbf{T}_{CLS} are the T-parameters for cross-line open circuited and short circuited, respectively. After the de-embedding the remaining responses are \mathbf{T}_{CLO}^4 and \mathbf{T}_{CLS}^4 which can be easily solved for \mathbf{T}_{CLO} and \mathbf{T}_{CLS} , the remaining responses are illustrated in Fig. 3(a) and (b) respectively. In order to continue for characterization, the additional transmission lines from both sides for the two cases have to be de-embedded. Only terminated cross-line results remain, which can be represented with S-parameter matrices as \mathbf{S}_{CO} and \mathbf{S}_{CS} . The S-parameters can be provided in detail using Eq. (1) and (2) as follows;

$$S_{CO,11} = S_{11} + \frac{[(1-S_{11})(S_{21}^2+S_{31}^2)+2S_{21}S_{31}S_{41}]}{(1-S_{11})^2-S_{41}^2} \quad (9)$$

$$S_{CO,21} = S_{41} + \frac{[2S_{21}S_{31}(1-S_{11})+S_{41}(S_{21}^2+S_{31}^2)]}{(1-S_{11})^2-S_{41}^2} \quad (10)$$

$$S_{CS,11} = S_{11} + \frac{[-(1+S_{11})(S_{21}^2+S_{31}^2)+2S_{21}S_{31}S_{41}]}{(1+S_{11})^2-S_{41}^2} \quad (11)$$

$$S_{CS,21} = S_{41} + \frac{[-2S_{21}S_{31}(1+S_{11})+S_{41}(S_{21}^2+S_{31}^2)]}{(1+S_{11})^2-S_{41}^2} \quad (12)$$



Fig. 3. Remaining responses after de-embedding and solving for one structure (a) cross-line terminated ports with open circuit, and (b) cross-line terminated ports with short circuit.

The four unknowns (S_{11} , S_{21} , S_{31} , and S_{41}) of cross-line can be calculated using known values of $S_{CO,11}$, $S_{CO,21}$, $S_{CS,11}$, and $S_{CS,21}$ and using Eqs. (9)-(12). The equations for unknowns are given below.

$$S_{CO,T} = S_{CO,11} + S_{CO,21} \quad (13)$$

$$S_{CS,T} = S_{CS,11} + S_{CS,21} \quad (14)$$

$$S_{CO,D} = S_{CO,11} - S_{CO,21} \quad (15)$$

$$S_{CS,D} = S_{CS,11} - S_{CS,21} \quad (16)$$

$$C_1 = (S_{CO,T} + S_{CS,T}) / (2 + S_{CO,T} - S_{CS,T}) \quad (17)$$

$$C_2 = (S_{CO,D} + S_{CS,D}) / (2 + S_{CO,D} - S_{CS,D}) \quad (18)$$

$$S_{11} = (C_1 + C_2) / 2 \quad (19)$$

$$S_{41} = (C_1 - C_2) / 2 \quad (20)$$

$$C_3 = \sqrt{(S_{CO,T} - S_{CS,T})(1 - C_1^2) / 2} \quad (21)$$

$$C_4 = \sqrt{(S_{CO,D} - S_{CS,D})(1 - C_2^2) / 2} \quad (22)$$

$$S_{21} = (C_3 + C_4) / 2 \quad (23)$$

$$S_{41} = (C_3 - C_4) / 2 \quad (24)$$

Using Eqs. (13) through (24), the four unknown S-parameters of cross-line can be calculated. In the next section the results of this method with a comparison are provided.

IV. EXPERIMENTAL RESULTS

The method described above is followed and the unknown S-parameters of cross-line is calculated from the two-port measurements. The results are presented in Fig. 4(a)-(h) in red lines in comparison with the S-parameters calculated from four-port measurements with the method described in [2] represented with blue lines. The results from two-port measurements are calculated up to 110 GHz, while the results calculated from four-port measurements are up to 67 GHz since the four-port VNA works up to this frequency. As it can be observed from Fig. 4(a) and (b) that the return loss results are very close to each other, except there is some difference after 50 GHz both in magnitude and phase. S_{21} magnitude is very close for the two cases, and the phase is different than each other. Similarly, S_{31} magnitude are in good agreement, however there is difference after 40 GHz. The phase is also different in the overall frequency region. On the other hand, insertion loss, which is S_{41} , well-matched in magnitude, and a little difference in phase domain. The reason of the difference between S_{21} and S_{31} is because of the coupling effects on the four-port measurements. These comparisons shows that the method is accurate.

V. CONCLUSION

An electrically symmetrical and reciprocal four-port cross-line, used in differential cross coupled amplifiers for decreased amplitude and phase imbalance, are characterized up to 110 GHz using two-port measurements accurately. The method for characterization along with the characterization structures are introduced in this paper. In order to validate the results of method, the calculated S-parameters are compared with the S-parameters calculated using four-port measurements [2]. The comparisons show that the method is very accurate. Such that, one can use the model even after 67 GHz even there is no differential measurements are done.

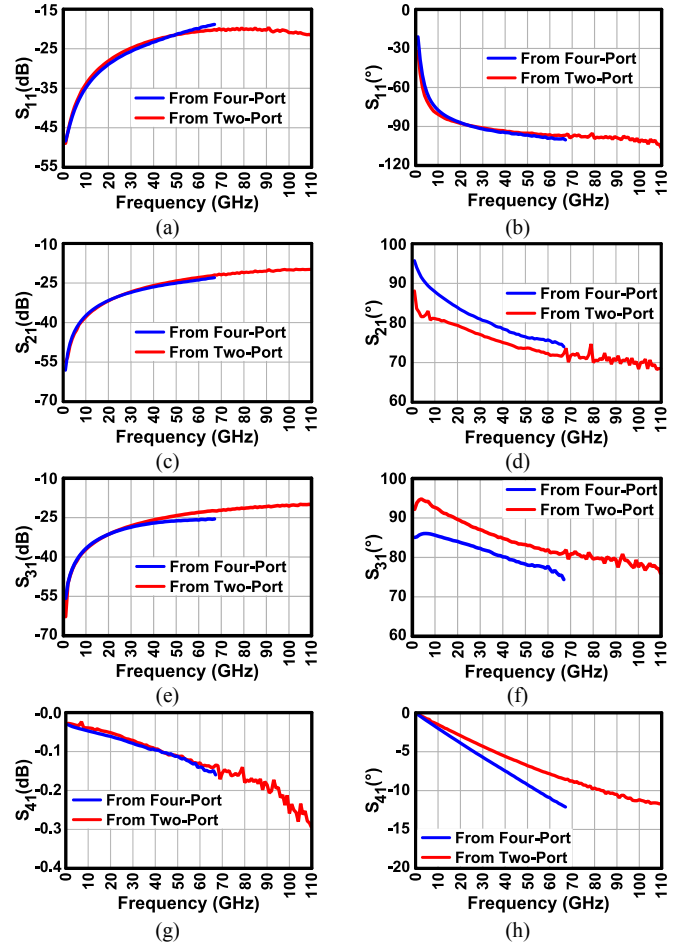


Fig. 4. Cross-line S-parameter comparison between calculated from four-port measurements [2] (blue lines), and from two-port measurements of the proposed method (red lines), (a) magnitude of (return loss) S_{11} , (b) phase of S_{11} , (c) magnitude of S_{21} , (d) phase of S_{21} , (e) magnitude of S_{31} , (f) phase of S_{31} , (g) magnitude of (insertion loss) S_{41} , and (h) phase of S_{41} .

ACKNOWLEDGMENT

This work is partially supported by MIC, SCOPE, MEXT, STARC, STAR, and VDEC in collaboration with Cadence Design Systems, Inc., Mentor Graphics, Inc., and Keysight Technologies Japan, Ltd.

REFERENCES

- [1] K. Okada *et al.*, "A 64-QAM 60 GHz CMOS Transceiver with 4-Channel Bonding," ISSCC, San Francisco, CA, pp. 346-347, Feb. 2014.
- [2] K. K. Tokgoz, K. Lim, Y. Seo, S. Kawai, K. Okada, and A. Matsuzawa, "Cross-Line Characterization for Capacitive Cross Coupling in Differential Millimeter-Wave CMOS Amplifiers," IEEE SiRF 2015, San Diego, CA, pp. 46-48, Jan. 2015.
- [3] K. K. Tokgoz, K. Lim, S. Kawai, N. Fajri, K. Okada, and A. Matsuzawa, "Characterization of Crossing Transmission Line Using Two-Port Measurements for Millimeter-Wave CMOS Circuit Design," IEICE Trans. Electron., vol. E98-C, no. 1, pp. 35-44, Jan. 2015.
- [4] C. J. Chen and T. H. Chu, "Virtual Auxiliary Terminations for Multi-Port Scattering Matrix Measurement Using Two-Port Network Analyzer," IEEE MTT, vol. 55, no. 8, pp. 1801-1810, Aug. 2007.
- [5] S. Kawai, K. K. Tokgoz, K. Okada, and A. Matsuzawa, "L-2L De-embedding Method with Double-T-Type Pad Model for Millimeter-Wave Amplifier Design," IEEE SiRF 2015, San Diego, CA, pp. 43-45, Jan. 2015.